

Article

Thermal Performance of Alginate Concrete Reinforced with Basalt Fiber

Seyed Esmaeil Mohammadyan-Yasouj ^{1,*}, Hossein Abbastabar Ahangar ²,
Narges Ahevani Oskoei ¹, Hoofar Shokravi ³, Seyed Saeid Rahimian Koloor ⁴
and Michal Petru ⁴

¹ Department of Civil Engineering, Najafabad Branch, Islamic Azad University, Najafabad 8514143131, Iran; narges.oskoei@yahoo.com

² Department of Chemistry, Najafabad Branch, Islamic Azad University, Najafabad 8514143131, Iran; abbastabar@gmail.com

³ School of Civil Engineering, Faculty of Engineering, Universiti Teknologi Malaysia, Skudai 81310, Johor, Malaysia; shoofar2@graduate.utm.my

⁴ Institute for Nanomaterials, Advanced Technologies and Innovation (CXI), Technical University of Liberec (TUL), Studentska 2, 461 17 Liberec, Czech Republic; s.s.r.koloor@gmail.com (S.S.R.K.); Michal.petru@tul.cz (M.P.)

* Correspondence: sm7093370@yahoo.com

Received: 13 July 2020; Accepted: 28 August 2020; Published: 3 September 2020



Abstract: The sustainability of reinforced concrete structures is of high importance for practitioners and researchers, particularly in harsh environments and under extreme operating conditions. Buildings and tunnels are of the places that most of the fire cases take place. The use of fiber in concrete composite acts as crack arrestors to resist the development of cracks and enhance the performance of reinforced concrete structures subjected to elevated temperature. Basalt fiber is a low-carbon footprint green product obtained from the raw material of basalt which is created by the solidification of lava. It is a sustainable fiber choice for reinforcing concrete composite due to the less consumed energy in the production phase and not using chemical additives in their production. On the other hand, alginate is a natural anionic polymer acquired from cell walls of brown seaweed that can enhance the properties of composites due to its advantage as a hydrophilic gelling material. This paper investigates the thermal performance of alginate concrete reinforced with basalt fiber. For that purpose, an extensive literature review was carried out then two experimental phases for mix design and to investigate the compressive strength of samples at a temperature range of 100–180 °C were conducted. The results show that the addition of basalt fiber (BF) and/or alginate may slightly decrease the compressive strength compared to the control concrete under room temperature, but it leads to control decreasing compressive strength during exposure to a high temperature range of 100–180 °C. Moreover, it can be seen that temperature raise influences the rate of strength growth in alginate basalt fiber reinforced concrete.

Keywords: concrete; sodium alginate; basalt fiber; compressive strength; temperature

1. Introduction

Concrete is widely used in the construction of many structures such as buildings [1,2] and bridges [3,4]. Plain concrete is weak in tension due to its brittle nature; hence fibers are added to sustain stresses and restrict the propagation of cracks [5]. There are various fibers used in concrete application that the most predominant types include synthetic, natural, carbon, glass, and steel [6]. Basalt fiber (BF) is a new kind of natural fiber manufactured from the extrusion of basalt rock in a melting temperature between 1500 and 1700 °C [7]. Basalt fibers have good resistance to fire and corrosion with advanced vibration and acoustic insulation capacity [8]. Basalt fiber is a cheaper and more eco-friendly alternative

to glass, carbon, or aramid fiber for reinforcing concrete composite due to the less consumed energy in the production phase and not using chemical additives in their production [9]. Table 1 shows a summary of previous studies that investigated the behavior of basalt fiber-reinforced concrete (FRC) compared with other fibers including polypropylene, glass, and polyvinyl alcohol (PVA).

Several experiments were conducted to study the effect of using different lengths, diameters, and proportions of fibers in concrete. Jiang et al. [10] studied the effect of BF on the mechanical characteristic of the FRC. The obtained results indicated that adding BF can significantly enhance the flexural and tensile strength, as well as the toughness index of FRC where no obvious increase of compressive strength was reported. In comparison to other fiber types, higher splitting tensile and flexural strengths of BF than polypropylene [10], higher tensile strength, crack resistance, and ductility and lower flexural strength of BF than glass fiber (GF) [11], lower increase in energy absorption at high strain rate by BF than GF [12], neutral contribution of BF and significant contribution of PVA in post cracking flexural response [13] have been reported. Almost all previous research on the fiber reinforced concrete confirmed that increase in the fiber length and/or content decreases concrete workability and increases its porosity [14]. Reduction in the workability due to an increase in the fiber content requires higher water to cement ratio which leads to higher porosity in the hardened concrete. Accordingly, fiber content is also a main parameter considered by previous researchers to control the fiber effect on the concrete properties. However, selecting an appropriate amount of fiber content to reach proper workability with expected mechanical properties for concrete is necessary.

Alginate sodium is a biopolymer extracted from cell walls of brown algae, that forms swollen hydrogels in the presence of water [15,16]. It is a linear anionic polysaccharide composed of mannuronic (M) and guluronic (G) acid that is glycosidically connected via α -1 \rightarrow 4 and β -1 \rightarrow 4 linkages thus hydrogel formation occurs through ionic cross-linking [17]. Sodium alginate is currently being investigated for the production of self-healing of concrete [18]. Alginate concentration influences the properties of the produced hydrogel [19]. Abbas and Mohsen [20] investigated the effect of alginate in the behavior of concrete. It is reported that the addition of alginate increased the slump and fresh density, and improved the workability of fresh concrete. Enhanced mechanical properties (compressive, splitting tensile and flexural strength) were also reported by the addition of 1% of the alginate in the concrete mixture. However, Heidari et al. [21] indicated that alginate may decrease the mechanical properties of concrete, but some observations can improve the performance of self-compacting concrete in a fresh state. There are remarks that alginate gel releases its entrained mixing water and incites the densification and more hydration of cement particles [22]. Alginates also exhibit different thermal behavior according to the type used and alginate or its derivative were stated for their self-healing effect in concrete [23]. From the same resource, it was reported that building materials containing sodium alginate and/or calcium alginate lead to significant flame-, fire-, and heat-resistance or imperviousness to the materials. Due to these reports, alginate is promising for internal curing, self-sealing, and self-healing of cracks and is also effective when a high amount of superabsorbent is required. Though, the application of appropriate amounts of alginate in concrete or PC may help improving concrete characteristics such as its crack resistance or density that are effective for long term behavior. Table 4 shows a summary of the studies using alginate in concrete mixtures.

Table 1. Cement concrete with fiber.

Ref.	Conducted Tests and Sample Monitoring	Test Age (day)	Codes and Sample Size (mm)	Fiber Type			Remarks	
				Amount (% of the Total Volume)	Diameter (μm)	Length (mm)		Name
Jiang et al., 2014 [10]	Compression	3-7-28-90	\varnothing AS (1012.9-1999, 1012.10-2000, and 1012.11-1985)	(0.05, 0.1, 0.3, and 0.5)	20	12 and 22	Basalt (B)	Addition of fiber increased porosity and reduced workability
	Tension		100 \times 200 cylinder					Small to moderate increase in compressive strength (by BF > by PP) at 7–28 day age.
	Flexure		150 \times 300 cylinder					Higher toughness and splitting tensile strength (BF > PP) is achieved by increasing fiber contents.
	Permeability		75 \times 75 \times 305 prism					Addition to 0.3% fiber increases flexural strength; 0.5% BF content reduce flexural strength.
					-	4–19	Polypropylene (PP)	0.3% of BF content with the length of 22 mm increases tensile and flexure strength.
Kabay 2014 [24]	Compression	28	\varnothing EN 12390-3 and ASTM C642	(0.07 and 0.14)	13–20	12 and 24	B	Workability is reduced by increasing the length and/or volume of fibers.
	Flexure		71 \times 71 cube					Compared to compressive strength abrasion has a higher correlation with void content and flexural strength.
	Fracture energy		100 \times 100 cube					Addition of fiber reduced compression strength.
			70 \times 70 \times 285 prism (with 30 mm depth and 3 mm thickness notch)					The addition of fibers reduces abrasive wear in the range of 2–18%.
								Most improved flexure strength was seen in mixture with 60% w/c.
Ayoub et al., 2014 [25]	Compression	28-7	\varnothing BS (1881-125: 1986, 1881-3:1970, 1881-102)	(1, 2, and 3)	18	25	B	Increased BF contents reduced compressive strength.
	Tension		100 \times 200 cylinder					Higher tension strength is achieved for high-performance concrete with BF and 10% silica.
	E-value							BF does not correlate with E-value.
Kizilkanat et al., 2015 [11]	Compression	28-7	EN 12390-3, ASTM (C469M, C496), and JCI-S-002	(0.25, 0.5, 0.75, and 1)	13-20	12	B	Increasing fibers caused a significant increase in fracture energy where workability and E-value were decreased
	Tension		150 \times 150 \times 150 cube					Slight increase in compressive strength was observed in >0.25% fiber content

Table 1. Cont.

Ref.	Conducted Tests and Sample Monitoring	Test Age (day)	Codes and Sample Size (mm)	Fiber Type			Remarks
				Amount (% of the Total Volume)	Diameter (μm)	Length (mm)	
Fenu et al., 2016 [12]	Flexure	28	100 × 200 cylinder	3 and 5	13	12	0.5% and 0.75% inclusion of BF improved compressive strength
	E-value		100 × 100 × 350 prism (with 30 mm notch)				BF has a higher impact on crack avoidance and tensile strength and ductility
	Fracture energy						GF is directly related with flexure strength
	Compression		Ø EN (197-1, 196-1)				Fibers' addition did not show a significant impact on the dynamic increase factor.
	Tension		40 × 40 × 160 prism (cut from bending);				A significant and slight increase in energy absorption at a high strain rate was achieved by GF and BF respectively.
Flexure	100 × 200 cylinder core from prism for dynamic test	Improved static flexural strength and post-peak behavior were achieved by GF and BF.					
	SEM				14	12	G
Shafiqh et al., 2016 [13]	Flexure	28	Ø ASTM C192/C192M, C 494-86 Type G, C78, C 1609)	1, 2, and 3	18	25	Strain attaining capacity was achieved by the addition of GF and BF.
	SEM		100 × 200 × 1500 prism				Ductility post-cracking flexural response and toughness were significantly improved by PVA fibers.
Girgin 2016 [26]	Compression	17 and 28	Ø EN (1170-4/5:1997, 12467)	2	14–20	24	Stress accumulation due to the cement hydration in the matrix–fiber interface influenced flexural strain capacity of BF.
	Flexure		50 × 50 cube				A 35% reduction in the average strain capacity of GF-reinforced concrete compared with the 7-day one was achieved.
	Heating		12 × 600 × 600 square sheet				
	SEM		11 × 50 × 270 square sheet				

Table 1. Cont.

Ref.	Conducted Tests and Sample Monitoring	Test Age (day)	Codes and Sample Size (mm)	Fiber Type			Remarks	
				Amount (% of the Total Volume)	Diameter (μm)	Length (mm)		Name
Afroz et al., 2017 [9]	Compression		\varnothing AS (3972, 3582.1–1998, 1012.8, 1012.9, 1012.10, 1012.11)	0.5	15	3	B (Chinese)	Long-term compatibility of BF reinforcement fibers for chloride and sulfate solutions.
	Tension		100 \times 200 cylinder					Compared to non-modified BF modified BFs had better stability in alkaline medium.
	Flexure		150 \times 300 cylinder					Coating provided good protection while exposure to extensive alkaline ions from a physiochemical analysis point of view.
	SEM		100 \times 100 \times 350 prism					A reduction in the mechanical properties of concrete for treated fibers was observed.
	EDX							Improved long-term flexural strengths and splitting tensile for high volume fly ash concrete with silane coated BFs even after 56 days. Difference in compressive strength was not notably improved.
Zhao et al., 2017 [27]	Impact	120	GB/T 50082-2009	1, 1.5, 2, and 2.5	15	18	B	Gradual loss in performance was observed by freeze-thaw cycles.
	Freeze-thaw		40 \times 40 \times 160 prism					Improved anti-impact deformation characteristics were achieved using BF.
								Anti-impact deformation characteristics were weakened by freeze-thaw cycles.
Katkhuda and Shatarat 2017 [28]	Compression	28	\varnothing ASTM (C33, C127, C131, C1524, C143)	0.1, 0.3, 0.5, 1, and 1.5	16	18	B	Flexural and splitting tensile strength of BF-reinforced concrete was significantly improved while it was minimally enhanced for the compressive strength.
	Tension		100 \times 100 cube					The optimum BF content to achieve the same compressive and splitting tensile strength as the natural aggregate was 0.5% for untreated recycled coarse aggregate (RCA) and 0.3% for treated RCA while the optimum BF content for flexural strength was 0.3% for untreated RCA and 0.1% for treated RCA.
	Flexure		150 \times 300 cylinder					
	Permeability		100 \times 100 \times 500 prism					
Sun et al., 2019 [29]	Compression	28	\varnothing SL352-2006, CECS13:2009	1, 2, 3, 4, and 5	17.4	6 and 12	B	The compressive and splitting tensile strengths of concrete reduced with the increase of fiber content while the bending strength increased.
	Tension		150 \times 150 cube					Compared to BF with the length of 12 mm 6 mm BF had better splitting tensile performance and compressive strength while variation of bending strength is slight
	Flexure		100 \times 100 \times 400 prism					2% of 6 mm BF achieved the maximum strength

Using low carbon footprint materials as a constituent of concrete is one of the ways to improve the sustainability of the construction industry. Basalt fiber and alginate are two low carbon footprint green products that are widely used for improving the performance of the produced concretes. Recently, several studies have been carried out to investigate the effect of BF-reinforced concrete exposure to elevated temperature. Few researchers have covered the effect of alginate in concrete. To the best of the authors' knowledge, no research has been directed at determining the thermal performance of alginate concrete reinforced with basalt fiber. In this study, the effect of simultaneous and separate addition of BF and alginate to improve the temperature resistance of concrete is experimentally studied. A two stage procedure was used to carry out the experimental study. The first stage was conducted to determine the appropriate water to cement ratios and also deciding for inclusion or exclusion of the aggregate smaller than 150 μm (passed through sieve No. 100). In the second stage, the thermal performance of the mortar with addition or/and elimination of ingredients (alginate and basalt fiber) in the composition mix was investigated. Basalt fiber is expected to potentially enhance concrete's resistance to crack and prevent the damages such as spalling in the concrete caused by elevated temperatures. Sodium alginate is intended to improve the microstructure of concrete to achieve higher temperature resistance capacity while exposed to elevated temperature.

2. Materials and Methods

2.1. Materials

Materials including limestone aggregates, cement, BF, and alginate were purchased from local suppliers and prepared for mixtures. Type I Portland cement was used for concretes. Type I Portland cement was used for concretes. In the primary study on the prepared materials, the mix designs were investigated with 450 and 470 kg/m^3 cement amounts and 0.5 and 0.55 water to cement ratios. The aggregates for the mortar were crushed limestone and sieved below through sieve number 4 to provide relatively fine aggregates of sizes less than 4.75 mm in accordance of ASTM C117 and E11. The fineness modulus of the aggregates was determined to be 2.72. The size distribution curve for the aggregates is shown in Figure 1. The curve is in accordance to the standard area of ASTM C33-03. Water absorption of the aggregates was about 1%.

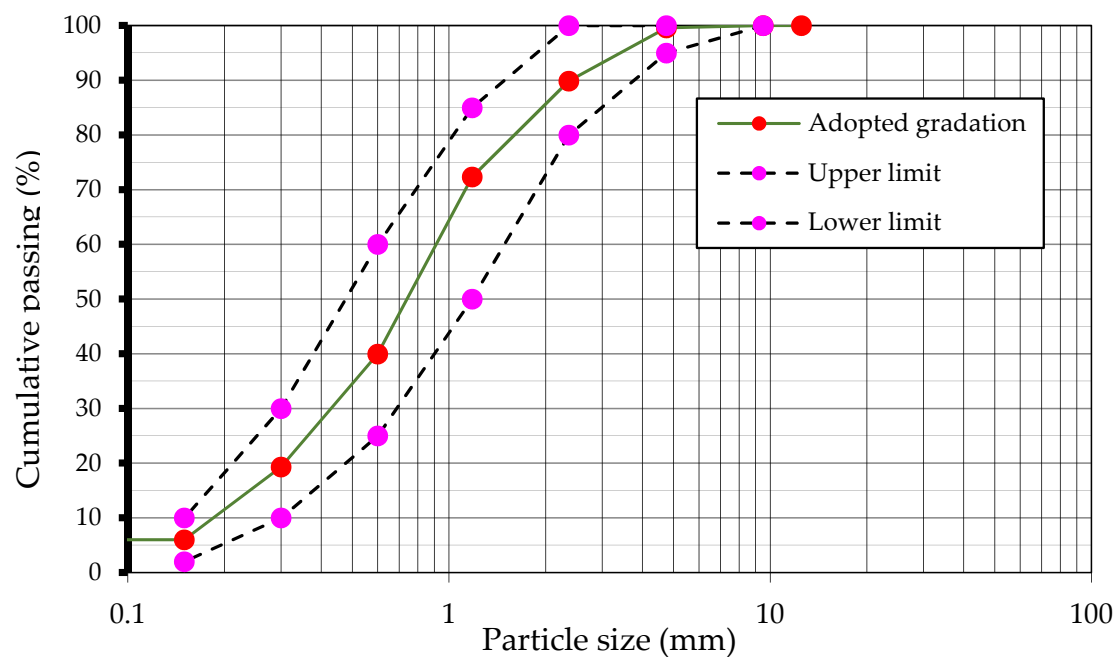


Figure 1. Size distribution curve for aggregate used in the present research.

Cubic mortar specimens of $50 \times 50 \times 50$ mm were cast for testing compressive strength. The maximum size of aggregates in the mortar was limited to the aggregates smaller than 4.75 mm (passed sieve No. 4), and fineness modulus was 2.72. From Table 1, it can be seen that the length of BF used for concrete-reinforcing applications in earlier studies was varied in the range of 3–30 mm. It is evident that shorter chopped fibers can achieve more uniform distribution while longer chopped lengths are more efficient in bridging and controlling the width of cracks. As shown in Table 1, in previous studies the amount of fiber content in concrete mixes varied in the range of 0.05–5% of the total concrete volume. The findings drawn from previous studies suggest using fiber content and a chopped length of 2% and 10 mm, respectively. From Table 2, the amount of sodium alginate used in concrete mixture is within a limited range. In this study, a sodium alginate concentration of 0.1% of the total mortar volume was used for each mixture. The morphological and mechanical properties of the BF used as reinforcement of the mortar specimens in the present study are demonstrated in Table 3. Figure 2 presents the materials used in the composition of the mortar mixes of the experimental study.



Figure 2. The materials used in the composition of the concrete mixes of the experimental study that includes (a) aggregate (b) cement (c) basalt fibers (d) alginate powder.

Table 2. Alginate application in concrete.

Ref.	Conducted Tests and Sample Monitoring	Test Age (day)	Codes and Sample Designation (mm)	Details on Alginate		Remarks
				Amount (% of Cement Weight)	Type	
Ouwere et al., 1998 [19]	E-value	1	Solution	-	Alginate gel bead	Alginate concentration limits the elasticity of breads.
	SEM					Properties of alginate gel bead are dependent on the concentration and polymer type.
Pathak et al., 2008 [16]	TGA	-	Solution	-	Dried algae (Sea mustard)	Alginic acid and metal alginates were prepared from fresh algae using extraction method then compared.
	FTIR					Conversion of alginic acid into metal alginate was confirmed by FTIR spectroscopy.
	DSC					Cobalt alginate became decomposed at a higher temperature in comparison to sodium and calcium alginate.
	SEM					Presence of metal ions impacted on pore size distribution of alginates.
	Porosity					Different thermal behavior was observed in different metal alginates due to the structural differences.
Heidari et al., 2015 [21]	Slump Flow (L-box)	7, 28, 56, and 90	Ø ASTM (C 462)	0.5 and 1	Alginic acid	Decrease in compressive, tensile, and flexural strengths by alginate.
	Compression		100 × 100 × 100 cube			Increase in workability, permeability, and compressive strength by silica.
	Tension		150 × 300 cylinder			Alginate improved performance of SCC in fresh state.
	Flexure		160 × 400 × 400 prism			In mixes containing alginate, nano and micro silica together, use of nano and micro-silica in upper percent of alginate increased the strength.
	Permeability					
Mignon et al., 2016 [22]	Compressive	28	Ø EN 196-1	0.5 and 1	Alginate biopolymers (NaAlg, CaAlg)	Alginate was promising for internal curing and was effective when much of superabsorbent polymer was required.
	Flexure		40 × 40 × 160 prism			NaAlg was insoluble due to the divalent cations in cement filtrate and created a physically cross-linked hydrogel.
	Swelling					CaAlg beads of 1% reduced only 15% of the compression strength.
						NaAlg of 1%, due to the higher water uptake capacity and stronger macro-pore, led to a 28% decrease in strength.

Table 3. Properties of basalt fiber (BF) used in the mortar specimens.

Cutting Length (mm)	10
Diameter (μm)	17
Density (gr/cm^3)	2.65
Elastic modulus (GPa)	93–110
Tensile strength (MPa)	4100–4800
Elongation (%)	1.3–3.2
Softening point ($^{\circ}\text{C}$)	1050
Water absorption (%)	<0.5

2.2. Mix Design and Specimen Preparation

The experimental study was carried out in two stages. The first stage consisted of six mixes considering two different water to cement ratios of 0.5 and 0.55 and also deciding for inclusion or exclusion of the aggregate smaller than $150\ \mu\text{m}$ (passed through sieve No. 100) identify water content and proportion of the mix. In the second stage, the main objective was to investigate the thermal performance of the mortar with addition and/or elimination of ingredients (alginate and basalt fiber) in the composition mix. Tables 4 and 6 present details on mix designs and the obtained compressive strength of each mix in the first stage, respectively. From the results in Table 6 that are discussed in the latter parts, $M_pW_{0.5}C_{470}E_{\#100}$ was considered as the reference mix design for concrete samples, in the second stage of the experiment.

Table 4. Details of mix designs in the primary study.

Name	Water–Cement Ratio	Cement (kg/m^3)	Polymer (%) *	Aggregates Passed Through Sieve # 100
$M_pW_{0.5}C_{450}I_{\#100}$ **	0.5	450	-	Included
$M_pW_{0.5}C_{470}I_{\#100}$	0.5	470	-	Included
$M_pW_{0.5}C_{450}E_{\#100}$	0.5	450	-	Excluded
$M_pW_{0.5}C_{470}E_{\#100}$	0.5	470	-	Excluded
$M_pW_{0.55}C_{450}E_{\#100}$	0.55	450	-	Excluded
$M_pW_{0.55}C_{470}E_{\#100}$	0.55	470	-	Excluded

* of the total weight. ** $M_pW_xC_yI_{\#z} > M_p$: mix design of the primary study, W_x : water to cement ratio of x , C_y : cement amount of $y\ \text{kg}/\text{m}^3$, $I_{\#z}$: represented inclusion of aggregate passed through the sieve number z in the mixture.

In the second stage, a different mix of BF and alginate was designed to be tested in various temperatures from room temperature to $180\ ^{\circ}\text{C}$ that is shown in Table 5. The compositions in the mix design were obtained based on the statistical design of the experiment. Moreover, it should be reminded that in the mix designs, the water to cement ratio and cement content was kept constant equal to 0.5 and $470\ \text{kg}/\text{m}^3$, respectively. The zero temperature in subsequent tables represent the room curing temperature without applying any external source of heating that is used as the reference before heating of samples. The compressive strength of the mixes was tested at several constant temperatures including 100, 150, and $180\ ^{\circ}\text{C}$. In order to test the compressive strength, of the samples in elevated temperature, the molds were opened after 24 h, and specimens were placed in a water tub for curing (ASTM C 109). After 28 days of water curing, the specimens were placed in the oven for 3 h under the intended temperature. After 3 h of heating, to prevent cooling shock, samples were not removed rapidly and the test was conducted after 24 h.

Table 5. Details of concrete composition in the main study.

Name **	BF (%) *	Alginate (%) *	Evaluation Temperature (°C)
MCT _{RT} ***	-	-	0
MCT ₁₀₀	-	-	100
MCT ₁₅₀	-	-	150
MCT ₁₈₀	-	-	180
MCBT _{RT}	0.2	-	0
MCBT ₁₀₀	0.2	-	100
MCBT ₁₅₀	0.2	-	150
MCBT ₁₈₀	0.2	-	180
MCAT _{RT}	-	0.1	0
MCAT ₁₀₀	-	0.1	100
MCAT ₁₅₀	-	0.1	150
MCAT ₁₈₀	-	0.1	180
MCBAT _{RT}	0.2	0.1	0
MCBAT ₁₀₀	0.2	0.1	100
MCBAT ₁₅₀	0.2	0.1	150
MCBAT ₁₈₀	0.2	0.1	180

* of the total weight. ** MCT, MCBT, MCAT, MCBAT are OC with no alginate and BF, with BF only, with alginate only, and with alginate and BF, respectively. *** RT represents room temperature.

2.3. Compressive Strength Testing

The compressive strength tests were according to ASTM C109-08. Mortar specimens were cast in triplicate cubic $50 \times 50 \times 50$ mm and tested for each mixture, after 28 days of water curing. Axial compressive load was applied to the specimen by a 3 MN capacity compressive testing machine. The compression load was applied continuously with a rate of 2.4 KN/s according to ASTM C31. The load was applied until the specimen reach its ultimate load-bearing capacity and failure occurred. Further discussion on behavior and mechanics of composites are provided in Cristescu et al. [30], Singh et al. [31], Abdi et al. [32], and Kolor and Tamin [33]. The stress and load were measured and recorded in MPa and KN, respectively. The failure patterns of the specimens under compressive load are given in Figure 3.

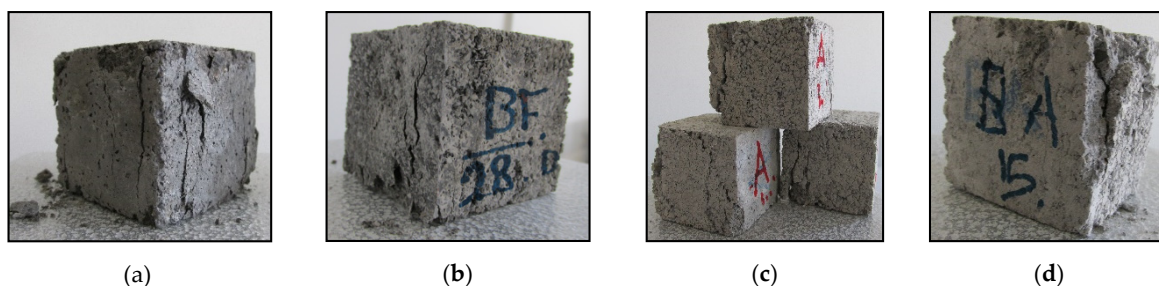


Figure 3. Failure pattern of samples under compression test (a) control sample, (b) BF-reinforced, (c) alginate mortar, (d) Alginate-BF mortar.

3. Results and Discussion

Figure 3 shows some of the specimens after failure under compression test. The investigation on the crack patterns of the specimens showed that the formation of cracks in non-fiber mortar samples was more compared to the ones in reinforced BF. It shows that the fibers act as the crack arrestors and block and divert crack formation and propagation. The failure of fiber concrete was gradual as compared to the abrupt and brittle failure of non-fiber concrete.

From Table 6, the highest compressive strength for samples of the mortars after 7 days was for mix design $M_pW_{0.5}C_{470}E_{\#100}$. Although the addition of the fine fraction of the aggregates passing through sieve No. 100 ($<150 \mu\text{m}$) may result in a richer Fuller curve gradation and achieving an optimum density and strength of the concrete mixture, the higher absorption capacity of the fine

particles necessitate an increase in w/c ratio that generally leads to a fall in the compressive strength. Higher compressive strength of $M_pW_{0.5}C_{470}E_{\#100}$ can be justified by the well-established fact that lower w/c ratio of mortar mixes gave rise to compressive strength.

Table 6. Compressive strength of primary tests.

Name	Age Tested	f'_c (MPa)
$M_pW_{0.5}C_{450}I_{\#100}$	7-day	29.9
$M_pW_{0.5}C_{470}I_{\#100}$		28.8
$M_pW_{0.5}C_{450}E_{\#100}$		30.6
$M_pW_{0.5}C_{470}E_{\#100}$		32.8
$M_pW_{0.55}C_{450}E_{\#100}$		23.0
$M_pW_{0.55}C_{470}E_{\#100}$		19.3

Results of compressive strength for the cement concrete samples are shown in Table 7, that are corresponding to four different temperature conditions.

Table 7. Compressive strength for the cement concrete.

Name	f'_c (MPa) 28-day	Variation to MCT ₀ (%)	Variation after Heating (%)		
MCT _{RT}	41.0	-	-	MCT _{RT}	Compared to
MCT ₁₀₀	34.0	-17.07	-17.07		
MCT ₁₅₀	31.9	-22.19	-22.19		
MCT ₁₈₀	35.6	-13.17	-13.17		
MCBT _{RT}	29.8	-27.32	-	MCBT ₀	Compared to
MCBT ₁₀₀	31.1	-24.15	+4.36		
MCBT ₁₅₀	30.1	-26.60	+1.01		
MCBT ₁₈₀	30.2	-26.34	+1.34		
MCAT _{RT}	27.6	-32.68	-	MCAT ₀	Compared to
MCAT ₁₀₀	33.7	-17.80	+22.10		
MCAT ₁₅₀	31.6	-22.93	+14.49		
MCAT ₁₈₀	28.2	-31.22	+2.17		
MCBAT _{RT}	24.4	-40.49	-	MCBAT ₀	Compared to
MCBAT ₁₀₀	28.2	-31.22	+15.57		
MCBAT ₁₅₀	23.4	-42.93	-4.10		
MCBAT ₁₈₀	22.6	-44.88	-7.38		

The compressive strength of the mixes compared to the reference mortar specimens maintained at room temperature are shown in Figure 4. The obtained results of the samples maintained at room temperature show that the addition of BF or alginate decreased compressive strength. A smaller reduction in compressive strength was observed by the addition of 0.2% of BF in the mortar mix, compared to the specimens containing alginate. The reduction of the compressive strength by the addition of BF is in agreement with the data published by other authors [24,25,29]. This decrease is mainly due to the compactness reduction of the composite caused by the introduction of voids into the matrix during incorporation of the fibers. However, the observation during compressive tests indicated that the specimens containing FB did not exhibit brittle failure but rather a ductile, plastic failure and the mortar showed the ability to absorb a large amount of plastic energy under compressive loads.

Hydrogels in alginate concrete can be formed by a crosslinking reaction of sodium alginate. The samples with sodium alginate pose higher water absorption capacity causing a greater amount of water to be required to achieve the desired workability compared to the control mortar. Lower workability contributes to making the concrete more porous and, as a consequence,

the compressive strength values would be decreased. On the other hand, releasing the encapsulated water in the mortar matrix as hydrogels leads to macropores which can reduce compactness of the composite and negatively affect the compressive strength. This result is in agreement with the findings of Heidari et al. [21] and Mignon et al. [22]. The application of both BF and alginate together decreased the compressive strength even more.

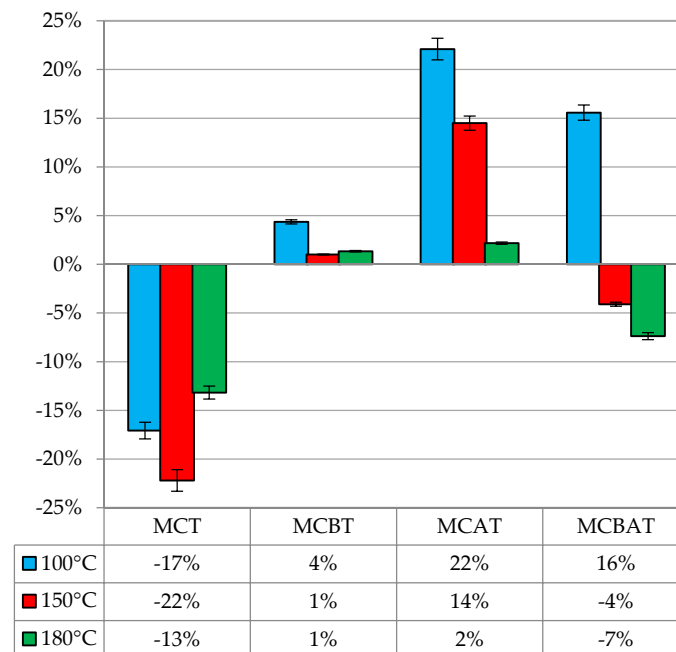


Figure 4. The compressive strength of the mixes compared to the reference mortar specimens maintained at room temperature.

Variations in the compressive strength of the mix designs after exposure to elevated temperature indicated that the maximum reduction of compressive strength for the control mixture was 22.19% when exposed to 100 °C for 3 h while the mix designs containing BF or alginate, each alone, even exhibited growth in the compressive strength. The maximum growth in the compressive strength was for MCAT₁₀₀; the composition containing sodium alginate subjected to 100 °C. After the introduction of water to sodium alginate, hydrogels are formed and they tend to cross-link in the presence of mixed metal oxides in the concrete that leads to dense structures after crosslinking and drying. The addition of the sodium alginate can efficiently encapsulate the dispersed micro or macro-size water droplets within the concrete composition. The encapsulated water droplets provide enhanced fire-resistive properties for the concrete. With increasing the temperature from 0 to 100 °C the encapsulated water is gradually released to facilitate the hydration of the cementitious system and positively influence the strength growth rate of the concrete.

It was observed that after 100 °C compressive strength was decreased. The reason for the decrease in compressive strength can be attributed to the effect of stress decay due to the viscoelastic relaxation of cross-linked alginate chains. Therefore, the internal hydrostatic pressures are developed and lead to water exudation through the network, as well as fracture of the air-containing cells, or to junction zones breakdown [34]. The mix design with BF has also revealed growth in the compressive strength after heating and the maximum growth in this mix design is under 100 °C too. These samples from mixed designs including BF or alginate exhibited small growth under 150 and 180 °C temperature. However, heating the cement concrete samples, including both BF and alginate subjected to 100 °C, resulted in compressive strength growth, but the increase of temperature to higher than 100 °C led to strength reduction. This reduction may be due to the departure of bound water in the microstructure and the free water from the cement past that results in concrete porosity. It can be attributed to the bonding

force between basalt fiber and the mortar matrix through the mechanical and chemical bonding. It must be mentioned that the bonding force decreases with increasing temperature [35].

4. Conclusions

In order to investigate the thermal performance of concrete and mortar containing alginate and BF, an experimental study was carried out. The variation in compressive strength of mortar mixes after exposure to an elevated temperature of 100, 150, and 180 °C was tested. The experimental program was performed in two stages including determination of the mix design of the control mix and afterward, investigating the thermal performance of the mortar with the addition and/or elimination of ingredients (alginate and basalt fiber) in the composition mix. The temperature variation can be divided into two ranges of 100 °C and temperatures beyond 100 °C in terms of effect on strength loss/gain. The mixes containing BF and alginate, or each alone, exhibited growth in the compressive strength when exposed to 100 °C due to enhanced hydration that exceeded the loss in strength. Basalt fiber and alginate are effective at stopping strength reduction of cement concrete under raised temperature. In view of these findings, it was concluded that the addition of BF and alginate results in an improved mortar that offers high temperature-resistive properties within the temperature range considered in the experiment.

Author Contributions: Conceptualization, N.A.O., S.E.M.-Y. and H.A.A.; methodology, N.A.O., S.E.M.-Y. and H.A.A.; software, N.A.O.; validation, N.A.O., S.E.M.-Y. and H.A.A.; formal analysis, N.A.O., S.E.M.-Y. and H.A.A.; investigation, N.A.O., S.E.M.-Y. and H.A.A.; resources, N.A.O., S.E.M.-Y., H.A.A., H.S., S.S.R.K. and M.P.; data curation, N.A.O.; writing—original draft preparation, N.A.O., S.E.M.-Y., H.A.A. and H.S.; writing—review and editing, N.A.O., S.E.M.-Y., H.A.A., H.S. and S.S.R.K.; visualization, N.A.O., S.E.M.-Y., H.A.A., H.S., S.S.R.K. and M.P.; supervision, S.E.M.-Y., H.A.A.; project administration, N.A.O., S.E.M.-Y., H.A.A., H.S., S.S.R.K. and M.P. funding acquisition, N.A.O., S.E.M.-Y., H.A.A., H.S., S.S.R.K. and M.P. All authors have read and agreed to the published version of the manuscript.

Funding: The research was funded by the Ministry of Education, Youth and Sports of the Czech Republic and the European Union (European Structural and Investment Funds—Operational Programme Research, Development and Education), Reg. No. CZ.02.1.01/0.0/0.0/16_025/0007293, as well as the financial support from internal grants in the Institute for Nanomaterials, Advanced Technologies and Innovations (CXI), Technical University of Liberec (TUL).

Acknowledgments: The authors would like to thank from Islamic Azad University, Najafabad Branch, for financial support, as well as facilities and services given and acknowledge the financial support by Ministry of Education, Youth and Sports of the Czech Republic and the European Union (European Structural and Investment Funds—Operational Programme Research, Development and Education), Reg. No. CZ.02.1.01/0.0/0.0/16_025/0007293, as well as the financial support from internal grants in the Institute for Nanomaterials, Advanced Technologies and Innovations (CXI), Technical University of Liberec (TUL).

Conflicts of Interest: The authors declare no conflict of interest.

References

1. Mohammadyan-Yasouj, S.E.; Marsono, A.K.; Abdullah, R.; Moghadasi, M. Wide beam shear behavior with diverse types of reinforcement. *ACI Struct. J.* **2015**, *112*, 199–208. [[CrossRef](#)]
2. Moghadasi, M.; Marsono, A.K.; Mohammadyan-Yasouj, S.E. A study on rotational behaviour of a new industrialised building system connection. *Steel Compos. Struct.* **2017**, *25*, 245–255. [[CrossRef](#)]
3. Shokravi, H.; Shokravi, H.; Bakhary, N.; Kolor, S.S.R.; Petrú, M. A Comparative Study of the Data-driven Stochastic Subspace Methods for Health Monitoring of Structures: A Bridge Case Study. *Appl. Sci.* **2020**, *10*, 3132. [[CrossRef](#)]
4. Shokravi, H.; Shokravi, H.; Bakhary, N.; Kolor, S.S.R.; Petrú, M. Health Monitoring of Civil Infrastructures by Subspace System Identification Method: An Overview. *Appl. Sci.* **2020**, *10*, 2786. [[CrossRef](#)]
5. Yuan, C.; Chen, W.; Pham, T.M.; Hao, H. Effect of aggregate size on bond behaviour between basalt fibre reinforced polymer sheets and concrete. *Compos. Part B Eng.* **2019**, *158*, 459–474. [[CrossRef](#)]
6. Ahmed, A.A.M.; Jia, Y. Effect of Using Hybrid Polypropylene and Glass Fibre on the Mechanical Properties and Permeability of Concrete. *Materials* **2019**, *12*, 3786. [[CrossRef](#)]

7. Alnahhal, W.; Aljidda, O. Effect of Fiber Volume Fraction on Behavior of Concrete Beams Made with Recycled Concrete Aggregates. In Proceedings of the MATEC Web of Conferences, 14 January 2019; EDP Sciences: Paris, France; Volume 253, p. 2004.
8. Swathi, T.; Resmi, K.N. Experimental Studies on Fly Ash Based Basalt Fibre Reinforced Concrete. In Proceedings of the 3rd National Conference on Structural Engineering and Construction Management, 15–16 May 2019; Springer: Kerala, India, 2019; pp. 25–39.
9. Wang, X.; He, J.; Mosallam, A.S.; Li, C.; Xin, H. The effects of fiber length and volume on material properties and crack resistance of basalt fiber reinforced concrete (BFRC). *Adv. Mater. Sci. Eng.* **2019**, *2019*. [[CrossRef](#)]
10. Jiang, C.; Fan, K.; Wu, F.; Chen, D. Experimental study on the mechanical properties and microstructure of chopped basalt fibre reinforced concrete. *Mater. Des.* **2014**, *58*, 187–193. [[CrossRef](#)]
11. Kizilkanat, A.B.; Kabay, N.; Akyüncü, V.; Chowdhury, S.; Akça, A.H. Mechanical properties and fracture behavior of basalt and glass fiber reinforced concrete: An experimental study. *Constr. Build. Mater.* **2015**, *100*, 218–224. [[CrossRef](#)]
12. Fenu, L.; Forni, D.; Cadoni, E. Dynamic behaviour of cement mortars reinforced with glass and basalt fibres. *Compos. Part B Eng.* **2016**, *92*, 142–150. [[CrossRef](#)]
13. Shafiq, N.; Ayub, T.; Khan, S.U. Investigating the performance of PVA and basalt fibre reinforced beams subjected to flexural action. *Compos. Struct.* **2016**, *153*, 30–41. [[CrossRef](#)]
14. Sarkar, A.; Hajihosseini, M. Feasibility of Improving the Mechanical Properties of Concrete Pavement Using Basalt Fibers. *J. Test. Eval.* **2020**, *48*. [[CrossRef](#)]
15. Mohammadyan-Yasouj, S.E.; Ghaderi, A. Experimental investigation of waste glass powder, basalt fibre, and carbon nanotube on the mechanical properties of concrete. *Constr. Build. Mater.* **2020**, *252*, 119115. [[CrossRef](#)]
16. Pathak, T.S.; San Kim, J.; Lee, S.-J.; Baek, D.-J.; Paeng, K.-J. Preparation of alginic acid and metal alginate from algae and their comparative study. *J. Polym. Environ.* **2008**, *16*, 198–204. [[CrossRef](#)]
17. Engbert, A.; Gruber, S.; Plank, J. The effect of alginates on the hydration of calcium aluminate cement. *Carbohydr. Polym.* **2020**, *236*, 116038. [[CrossRef](#)]
18. Wang, J.; Mignon, A.; Snoeck, D.; Wiktor, V.; Van Vlierberghe, S.; Boon, N.; De Belie, N. Application of modified-alginate encapsulated carbonate producing bacteria in concrete: A promising strategy for crack self-healing. *Front. Microbiol.* **2015**, *6*, 1088. [[CrossRef](#)]
19. Ouwerx, C.; Velings, N.; Mestdagh, M.M.; Axelos, M.A. V Physico-chemical properties and rheology of alginate gel beads formed with various divalent cations. *Polym. Gels Networks* **1998**, *6*, 393–408. [[CrossRef](#)]
20. Abbas, W.A.; Mohsen, H.M. Effect of Biopolymer Alginate on some properties of concrete. *J. Eng.* **2020**, *26*, 121–131.
21. Heidari, A.; Ghaffari, F.; Ahmadvand, H. Properties of self compacting concrete incorporating alginate and nano silica. *Asian J. Civ. Eng. BHRC* **2015**, *16*, 1–11.
22. Mignon, A.; Snoeck, D.; D'Halluin, K.; Balcaen, L.; Vanhaecke, F.; Dubruel, P.; Van Vlierberghe, S.; De Belie, N. Alginate biopolymers: Counteracting the impact of superabsorbent polymers on mortar strength. *Constr. Build. Mater.* **2016**, *110*, 169–174. [[CrossRef](#)]
23. DeBrouse, D.R. Alginate-Based Building Materials. U.S. Patent 8,246,733, 21 August 2012.
24. Kabay, N. Abrasion resistance and fracture energy of concretes with basalt fiber. *Constr. Build. Mater.* **2014**, *50*, 95–101. [[CrossRef](#)]
25. Ayub, T.; Shafiq, N.; Nuruddin, M.F. Mechanical properties of high-performance concrete reinforced with basalt fibers. *Procedia Eng.* **2014**, *77*, 131–139. [[CrossRef](#)]
26. Girgin, Z.C.; Yıldırım, M.T. Usability of basalt fibres in fibre reinforced cement composites. *Mater. Struct.* **2016**, *49*, 3309–3319. [[CrossRef](#)]
27. Zhao, Y.-R.; Wang, L.; Lei, Z.-K.; Han, X.-F.; Xing, Y.-M. Experimental study on dynamic mechanical properties of the basalt fiber reinforced concrete after the freeze-thaw based on the digital image correlation method. *Constr. Build. Mater.* **2017**, *147*, 194–202. [[CrossRef](#)]
28. Katkhuda, H.; Shatarat, N. Improving the mechanical properties of recycled concrete aggregate using chopped basalt fibers and acid treatment. *Constr. Build. Mater.* **2017**, *140*, 328–335. [[CrossRef](#)]
29. Sun, X.; Gao, Z.; Cao, P.; Zhou, C. Mechanical properties tests and multiscale numerical simulations for basalt fiber reinforced concrete. *Constr. Build. Mater.* **2019**, *202*, 58–72. [[CrossRef](#)]

30. Cristescu, N.D.; Craciun, E.-M.; Soós, E. *Mechanics of Elastic Composites*; CRC Press: New York, NY, USA, 2003; Volume 1, ISBN 0203502817.
31. Singh, A.; Das, S.; Craciun, E.-M. Effect of thermomechanical loading on an edge crack of finite length in an infinite orthotropic strip. *Mech. Compos. Mater.* **2019**, *55*, 285–296. [[CrossRef](#)]
32. Abdi, B.; Koloor, S.S.R.; Abdullah, M.R.; Amran, A.; Bin Yahya, M.Y. Effect of strain-rate on flexural behavior of composite sandwich panel. *Appl. Mech. Mater. Trans Tech. Publ.* **2012**, *229*, 766–770.
33. Koloor, S.S.R.; Tamin, M.N. Mode-II interlaminar fracture and crack-jump phenomenon in CFRP composite laminate materials. *Compos. Struct.* **2018**, *204*, 594–606. [[CrossRef](#)]
34. Mancini, M.; Moresi, M.; Rancini, R. Mechanical properties of alginate gels: Empirical characterisation. *J. Food Eng.* **1999**, *39*, 369–378. [[CrossRef](#)]
35. Wang, J.; Zhou, S.; Huang, J.; Zhao, G.; Liu, Y. Interfacial modification of basalt fiber filling composites with graphene oxide and polydopamine for enhanced mechanical and tribological properties. *RSC Adv.* **2018**, *8*, 12222–12231. [[CrossRef](#)]



© 2020 by the authors. Licensee MDPI, Basel, Switzerland. This article is an open access article distributed under the terms and conditions of the Creative Commons Attribution (CC BY) license (<http://creativecommons.org/licenses/by/4.0/>).